Phase-Modulated Stored Waveform Inverse Fourier Transform Excitation for Trapped Ion Mass Spectrometry

Ling Chen,[1] Tao-Chin Lin Wang,[1] Tom L. Ricca,[2] and Alan G. Marshall*[1,3]

Department of Chemistry, The Ohio State University, 120 West 18th Avenue, Columbus, Ohio 43210

The stored waveform inverse Fourier transform (SWIFT) technique offers a general method for exciting and/or ejecting ions having any range(s) of mass-to-charge ratios in either Fourier transform ion cyclotron resonance (FT/ICR) or ion-trap mass spectrometry. In this paper, we show that any of several types of nonlinear phase modulation (preferably, quadratic phase modulation) of the original frequency-domain spectrum before inverse Fourier transformation can successfully produce the desired low dynamic range in the time-domain as well as optimally flat frequency-domain transmitter power. Apodization of the time-domain waveform further smoothes the final excitation power profile. Phase-modulated SWIFT excitation is superior to currently available frequency-sweep excitation for enhanced mass resolution in mass spectrometry/mass spectrometry experiments, enhanced dynamic range and mass resolution via multiple-ion ejection of abundant ions, more uniform excitation magnitude for improved isotope-ratio measurements, multiple-ion simultaneous monitoring, and simultaneous excite/eject combinations. Theoretical and experimental results of various excitation methods are compared.

Fourier transform ion cyclotron resonance (FT-ICR) mass spectrometry (*1*, *2*) has advanced to become an extraordinarily versatile mass spectrometric technique offering ultrahigh mass resolution, simultaneous detection of the entire mass spectrum, and an upper mass limit that has yet to be reached (see reviews in Ref 3–10). Currently available excitation methods in FT-ICR are shown in Figure 1. Single-frequency excitation (top trace of Figure 1) was the method used to produce the very first FT-ICR spectrum (*1*) and is the principal excitation method in FT-NMR. However, as shown in Figure 1, top right, the "sinc" amplitude profile of this frequency-domain excitation spectrum is flat (to within a few percent) only over a small frequency range (ca. $\pm(0.1/T)$ Hz, in which T is the duration of the time-domain pulse). In general, single-pulse excitation producing nearly flat power over the full chemical mass range (i.e., a bandwidth of ca. 3 MHz at 3 T) would require a very short time-domain pulse (ca. 0.1 μs) of impractically large amplitude (>10^4 V, for a 1-in. plate separation) (*11*).

Therefore, a lower power (ca. 30 V (p-p)) frequency-sweep excitation technique (*2*) with detection after excitation has been adopted in all current FT-ICR instruments. However, the bottom trace of Figure 1 shows that the frequency-sweep excitation power spectrum is nonuniform in amplitude; moreover, the broad frequency rolloff on either side of the excitation spectrum limits the frequency selectivity; significant excitation power extends to about $(10/T)$ Hz (in which T is the duration of the frequency sweep) on either side of the desired band (*11*).

Broad-band excitation has also been achieved via pseudo-random (*12*) or random (*13*) noise as a spectral source. However, the resulting power spectrum is even more nonuniform than that from a frequency sweep, with comparably poor mass selectivity.

In order to achieve higher mass selectivity and a more uniform excitation power spectrum, we recently introduced a "tailored" excitation method, the stored waveform inverse Fourier transform (SWIFT) technique (*14*), illustrated in Figure 2 (top trace). In the SWIFT method, the time-domain excitation waveform applied to the transmitter plate is generated via digital-to-analog conversion of the inverse discrete Fourier transform of a specified discrete frequency-domain excitation magnitude spectrum. In theory, SWIFT should faithfully produce any desired discrete frequency-domain excitation/ejection power spectrum whose magnitude uniformity and mass selectivity are limited only by the duration of the time-domain signal (and thus by the size of the stored-waveform data set).

Figure 3 shows some possible SWIFT-generated excitation waveforms for application to FT-ICR experiments: flat power for wide band excitation; windowed excitation for suppression of selected ions; nonuniform power excitation to park ions of different m/z at different orbital radius; multiple-frequency excitation for multiple-ion monitoring or multiple-ion ejection; and multistep excitation power for simultaneous ejection of ions of selected m/z values and excitation of ions of other selected m/z value(s).

In previous papers (*14*, *15*) we demonstrated the use of SWIFT excitation for broad-band excitation, windowed excitation, multiple-ion-monitoring, and multiple-ion ejection for enhancement of dynamic range in FT-ICR. We also recognized that three major practical problems can arise from the potentially large time-domain dynamic range of a SWIFT waveform (Figure 2, top center diagram) generated by simple inverse Fourier transform of a specified discrete frequency-domain magnitude spectrum (*14*). First, the time-domain dynamic range may exceed the linear response range of the transmitter analog circuitry. Second, the necessary dynamic range may exceed the length (e.g., 20 bit) of the digital computer word needed to generate and store each time-domain voltage value. Third, because most of the transmitter power must be transmitted in such a short period, a much more powerful amplifier (ca. factor of 20 compared to broad band frequency-sweep excitation, in which the rf amplitude is constant during the excitation period) is needed. In this paper, we propose a general method for reducing the time-domain dynamic range of a SWIFT waveform, while preserving optimally uniform power and mass discrimination in the final frequency-domain excitation spectrum.

EXPERIMENTAL SECTION

SWIFT tailored excitation for FT-ICR mass spectrometry was first carried out with a modified Nicolet FTMS-1000 instrument in our laboratory (*14*). The desired time-domain waveform is stored in a separate 32-kiloword fast memory and clocked out via a 12-bit digital-to-analog converter to the transmitter circuit, as described in ref 15. Multiple excitation waveforms may be stored in different parts of the fast memory and recalled as needed for different stages of, e.g., an MS/MS experiment.

The SWIFT procedure begins by specifying the desired frequency-domain excitation magnitude spectrum at (e.g., 8K)

[1] Department of Chemistry.
[2] Campus Chemical Instrument Center.
[3] Department of Biochemistry.

0003-2700/87/0359-0449$01.50/0

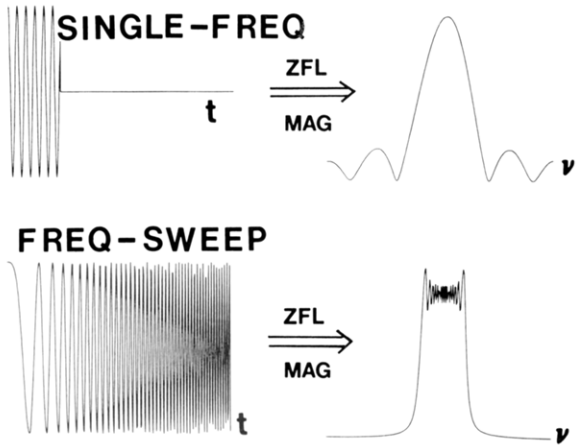

Figure 1. Prior FT-ICR excitation time-domain waveforms (left) and their corresponding frequency-domain spectra (right) obtained via Fourier transformation followed by magnitude-mode calculation (MAG) of a time-domain data set padded (ZFL) with an equal number of zeros: top, single-frequency pulse excitation (*1*); bottom, frequency-sweep excitation (*2*, *11*).

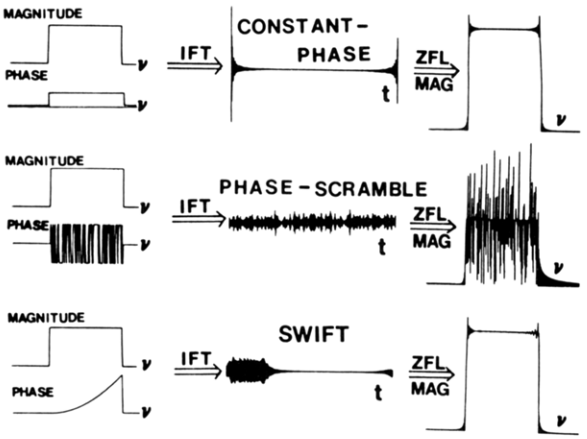

Figure 2. Effect of three different phase-encoding schemes upon excitation amplitude spectra. Frequency-domain spectra, specified by their magnitude and phase at each discrete frequency (left), are inverse Fourier transformed (IFT) to give their corresponding discrete time-domain waveforms (middle). After reflection about the time midpoint and one zero fill, forward Fourier transformation reveals the full magnitude-mode spectrum (right) both "at" and "between" the originally defined frequencies. The three schemes are as follows: (top row) zero-phase encoding of the specified excitation, yielding a relatively flat full spectrum (right), but at the cost of large dynamic range in the time domain (middle); (middle row) phase-encoding in which the phase is varied pseudorandomly (*12*) between $+\pi$ andd $-\pi$, resulting in greatly reduced dynamic range in the time-domain and flat magnitude *at* each defined point of the full frequency-domain spectrum, but exhibiting dramatic variation in the spectral magnitude *between* originally specified adjacent frequencies; (bottom row) phase-chirp encoding in which the phase varies quadratically with frequency, yielding both low dynamic range in the time-domain waveform and optimally flat magnitude in the full frequency-domain spectrum (even at frequencies between the originally specified frequencies).

discrete equally spaced frequencies. At this stage, in order to reduce the dynamic range of the subsequent time-domain waveform, a specified phase encoding is used to generate real and imaginary data sets (e.g., 8K each) whose magnitude spectrum remains unchanged from that originally specified. The resultant complex spectrum is then subjected to a complex inverse Fourier transform to generate a corresponding time-domain waveform. This time-domain profile is then reflected about its time midpoint in order to avoid sudden voltage transients at the beginning and end of the excitation period. The time-domain signal can (if desired) be apodized by multiplying it by a predefined weight function designed to bring the initial and final segments of the signal smoothly to zero. The final time-domain waveform is then normalized so that the largest values fall within the range (±2048)

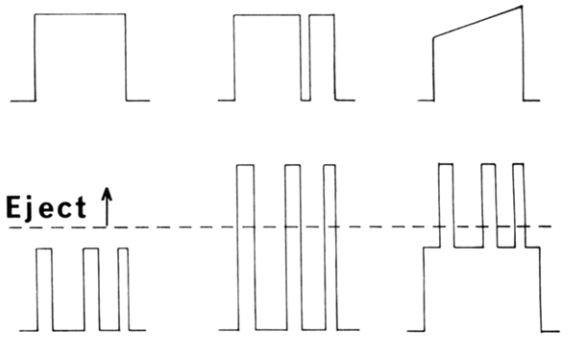

Figure 3. Representative excitation waveforms made possible by the SWIFT technique: (top, left to right), wide-band excitation with flat power, selective ion suppression, nonuniform excitation; (bottom, left to right), multiple-ion monitoring, multiple-ion ejection, simultaneous ejection/excitation.

spanned by the 12-bit digital-to-analog converter (DAC).

When two or more stored-waveform excitations are used in a single experimental event sequence (e.g., collision induced dissociation), each time-domain waveform and its corresponding parameters (event number, excitation mode, data array size, excitation amplifier gain, and excitation bandwidth (which specifies the DAC clock rate)) are temporarily stored in unused portions of core memory. The three possible excitation modes are as follows: direct-mode windowed excitation, in which the specified excitation spectrum extends from zero to the bandwidth; heterodyne-mode excitation, in which the stored-waveform signal is mixed with a radio frequency carrier signal to produce excitation extending as far as the specified bandwidth on either side of the carrier; and normal frequency-sweep excitation, in which the fast memory module is bypassed and the time-domain waveform is clocked out according to a programmed selection of data points from a quarter-wave sinusoid stored in 4K of core memory.

Once the excitation waveforms have been generated and stored, a simple subroutine (controlled by a three-letter command) loads the complete excitation sequence from core memory into proper locations in the separate 32-kiloword fast-memory module. It is worth noting that existing software commands can be used to setup the experimental parameters and event sequence (e.g., double resonance, triple resonance), up to a maximum (for the FTMS-1000) of six events. Of course, the event duration for each stored waveform excitation must be long enough that all of the stored-waveform values (e.g., $\geq 2(\mathrm{BWI})T$, in which BWI is the excitation bandwidth and T is the duration of the excitation period) can be clocked out during that period.

Finally, it is worth noting that a suitably phase-modulated SWIFT waveform (see below) requires an excitation amplitude only about twice as large (i.e., 3 dB) as that for a frequency-sweep spanning the same bandwidth. Therefore, it is not necessary to increase the gain of the transmitter amplifiers.

RESULTS AND DISCUSSION

Time-Domain Dynamic Range Problem. The origin of the large dynamic range in the time-domain waveform produced by constant-phase SWIFT (upper middle waveform Figure 2) lies in the common phase relation between all of the specified frequency-domain excitation spectral components. An inverse Fourier transform of a mathematically real frequency-domain spectrum (i.e., a spectrum in which the phase is zero at each frequency) yields a time-domain waveform composed of a sum of pure cosines (i.e., each sinusoidal component begins at a maximum at time zero). Thus, the SWIFT time-domain dynamic range problem arises because all of the specified frequency components begin with the *same phase* at time zero, much as in the centerburst in an FT-IR interferogram or the large initial signal in an NMR free induction decay (*16*).

Pseudorandom Phase Encoding. The obvious solution is to destroy the initial time-domain phase coherence by somehow scrambling the initial phases in the frequency-domain before inverse Fourier transformation. Our first idea,

by analogy to tailored (*17*) or stochastic (*18*) excitation in FT-NMR, was to scramble the initially specified frequency-domain phases pseudorandomly, as shown at the middle left of Figure 2. Pseudorandom phase scrambling succeeds in reducing the time-domain dynamic range (by a factor of about 20 for the broad band SWIFT example in the middle of Figure 2) and yields excitation power which is perfectly flat at the initially specified evenly spaced discrete frequencies.

However, since excitation and detection are temporally separated in FT-ICR (even with SWIFT), the excitation magnitude must be examined at *all* frequencies within the bandwidth, not just at the initially specified discrete frequencies. The excitation magnitude at frequencies evenly spaced between the initially specified frequencies is revealed by the magnitude-mode Fourier transform of a time-domain waveform to which an equal number of zeroes has been added (*19, 20*), as shown at the middle right of Figure 2. Although pseudorandomly phase-scrambled SWIFT excitation yields a power spectrum with constant magnitude at the initially specified frequencies, the magnitude is extremely nonuniform at intervening frequencies. Such nonuniform excitation power severely limits the utility of pseudorandomly phase-scrambled SWIFT excitation for broad-band FT-ICR *detection*, but the method is still suitable for multiple-ion *ejection* experiments in which the precise amount of power applied at a given m/z value is not critical as long as it exceeds the level required for ion ejection at that frequency.

Although tailored (stochastic) FT-NMR is based upon pseudorandom phase-modulated waveforms, excitation and detection are essentially simultaneous in that experiment. Thus, the spectral magnitude-fluctuation problem is never manifested because the response is detected at the same frequencies as the specified excitation, so that the intermediate frequencies are never sampled.

We have observed frequency-domain magnitude fluctuations (middle right of Figure 2) for a wide variety of phase-encoding schemes based on random or pseudorandom (e.g., maximal-length shift register) sequences, e.g., phase variation between π and $-\pi$, between 0 and π, between all values between 0 and π, and so on. The key feature appears to be the presence of *discontinuities* in the spectrum of phase vs. frequency. Therefore, one is next led to investigate phase modulation in which the phase varies *continuously* with frequency.

Linear Phase Variation and the Shift Theorem. The simplest nonconstant continuous phase function is a linear variation of phase with frequency. However, consideration of the shift theorem of Fourier analysis (*21*) quickly shows that prior linear phase encoding in the frequency domain will simply shift the time-domain waveform by an amount proportional to the rate of change of phase with frequency. Comparison of the top row of Figure 2 (phase is constant with frequency) and the top row of Figure 4 (phase varies linearly with frequency) confirms that linear phase encoding simply shifts the time-domain waveform without affecting the time-domain dynamic range.

Quadratic Phase Modulation. In principle, any nonlinear continuous phase modulation (i.e., nonconstant rate of change of phase with frequency) in the initially specified frequency-domain spectrum should succeed in reducing the corresponding time-domain dynamic range. Phase may be varied across the entire excitation bandwidth or (as in Figures 2 and 4) only across the segments of nonzero excitation magnitude. Although only quadratic phase modulation is discussed in this paper, cubic or higher-order polynomials can also be used.

Quadratic phase modulation is performed in the frequency-domain before inverse Fourier transformation. Real (cosine component) and imaginary (sine component) spectra (e.g., Figure 5, upper left) are calculated from the frequency-domain magnitude and phase, ϕ, at each frequency-domain data point (e.g., Figure 5, lower left)

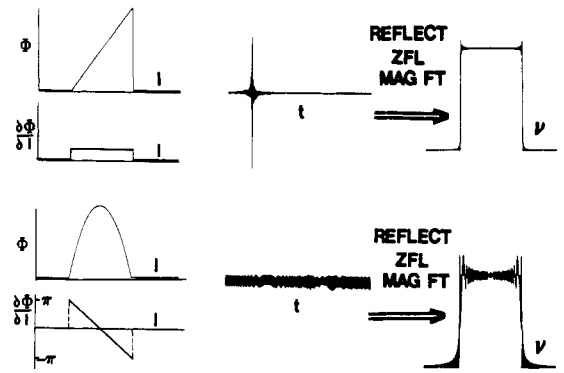

Figure 4. Excitation spectra (right) produced by frequency-domain phase modulation of a specified rectangular excitation spectrum. The frequency index, I, spans the frequency range within which the excitation magnitude is nonzero. The spectra are as follows: (top) linearly varied phase vs. frequency (upper left) and its first derivative with respect to frequency (lower left), time-domain waveform obtained by inverse Fourier transformation (middle), and the Fourier transform magnitude-mode spectrum (right) of the midpoint-reflected, zero-filled time-domain waveform; (bottom) as above, but for quadratic variation of phase with frequency (I).

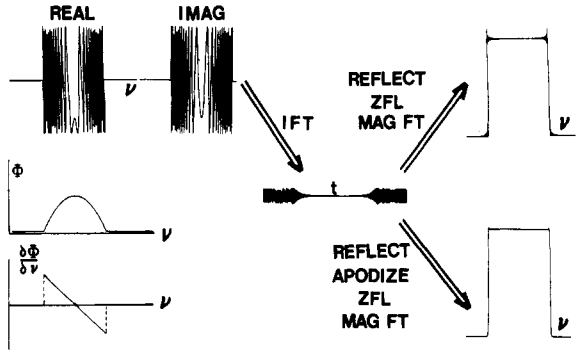

Figure 5. SWIFT with phase modulation. Quadratic phase encoding (middle left, along with its first derivative spectrum at lower left) of a specified rectangular excitation magnitude spectrum gives the real and imaginary spectra shown at upper left. Inverse Fourier transformation gives the time-domain waveform shown at the center of the figure, with excitation power spread over about half of the excitation period (middle). Forward Fourier transformation followed by magnitude-mode calculation of the midpoint-reflected (REFLECT), zero-filled (ZFL) time-domain waveform yields the full spectrum at upper right. Addition of an apodization step (see next figure) gives the somewhat smoother spectrum at lower right.

$$\text{real} = \text{magnitude}\cdot\cos\phi \quad (1a)$$

$$\text{imaginary} = \text{magnitude}\cdot\sin\phi \quad (1b)$$

Since frequencies are sampled at equally spaced intervals, we may represent ϕ_I vs. I as

$$\phi_I = \phi_0 + AI + (B/2)I^2 \quad (2)$$

in which the frequency index, I, spans a frequency range within which the excitation magnitude is nonzero, and the initial phase, ϕ_0, is chosen as zero at $I = 0$. For quadratic phase encoding, the phase rate of change is linear with frequency

$$\partial\phi_I/\partial I = A + BI \quad (3)$$

The quadratic phase encoding is conveniently characterized by its parameters, A and B. For example, $A = 0.5\pi$ and $B = -\pi/N_1$, in which N_1 is the number of nonzero data points in the synthesized frequency range in Figure 5.

Effect of Phase Modulation Rate upon Time-Domain Dynamic Range. Figure 4 (bottom row) illustrates one type of quadratic phase modulation. In the frequency domain, the

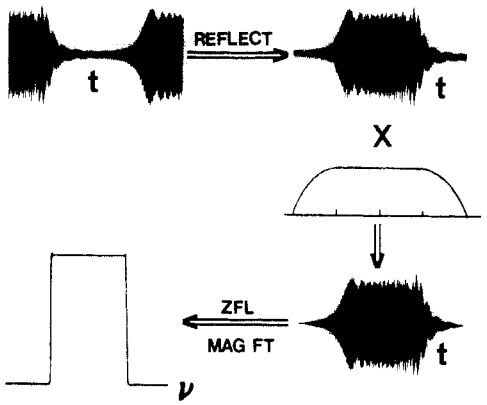

Figure 6. Effect of apodization of a SWIFT time-domain waveform. The apodization weight function (middle right) is a quarter-wave sinusoid at the first and last quarter of the time-domain period and is constant in between.

phase increases quadratically from 0 to 50π rad and then decreases quadratically back to 0, at a constant rate of change of phase with frequency. In accord with the Nyquist criterion (*16*) the maximum absolute rate of phase change cannot exceed π per frequency-domain data point. For quadratic phase modulation at rates approaching the Nyquist limit (Figure 4, bottom left), the excitation power is evenly distributed over the entire time-domain excitation period (Figure 4, bottom middle), yielding a time-domain dynamic range which is about the same as for frequency-sweep excitation and somewhat lower than for pseudorandom phase scrambling (compare to middle row of Figure 2). Unfortunately, the excitation magnitude full spectrum (Figure 4, bottom right) exhibits substantial nonuniformity, although not as severe as for pseudorandom phase-encoding (middle right of Figure 2).

Generally, we find that the objectionable nonuniformity (bottom right of Figure 4) can be removed if the rate of phase change is kept at half the Nyquist limit or below. For example, excitation magnitude full spectra based on quadratic phase modulation with a phase rate of change which varies from $+0.5\pi$ to -0.5π per data point (Figure 5, top right) or from 0 to $+0.5\pi$ per data point (Figure 2, bottom right) are essentially as flat as for constant-phase modulation (Figure 2, top right) but exhibit greatly reduced time-domain dynamic range compared to the constant-phase spectrum. There is evidently a trade-off between low dynamic range in the time domain and optimal magnitude uniformity in the frequency domain. As a rule of thumb, quadratic phase modulation with maximal phase rate of change at half the Nyquist limit appears to yield optimally flat frequency-domain excitation power at the expense of doubling the minimum possible time-domain dynamic range.

Apodization of the Excitation Waveform. Apodization (literally, removal of "feet", in reference to the auxiliary small peaks of a sinc line shape) of a time-domain signal is a well-known method for smoothing the frequency spectrum of a *response* (*16*). Here we discuss its use for smoothing the spectrum of an *excitation*. First, however, it is convenient to reflect the SWIFT-generated time-domain signal about its time midpoint, as shown in Figure 6. This procedure is equivalent to a time shift and, therefore, affects the phase but not the magnitude of the corresponding frequency-domain spectrum. The advantage of this procedure is that excitation power need not be turned on suddenly to a large value (as in Figure 6, upper left; Figure 2, bottom center; Figure 5, middle), thereby reducing problems from switching transients in the transmitter electronics.

A convenient apodization function (see Figure 6) consists of a quarter-wave sinusoid matched to one-fourth of the time-domain period, followed by unit weighting for the next

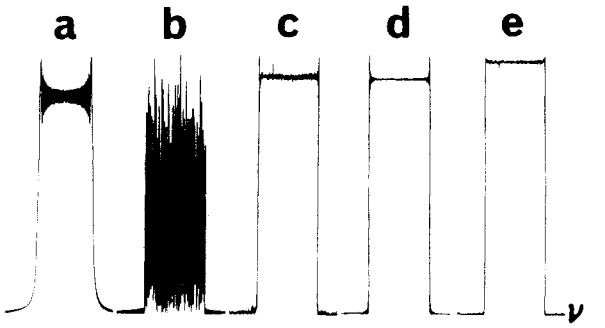

Figure 7. Experimental magnitude-mode excitation full spectra, obtained via Fourier transformation of a once zero-filled time-domain receive-during-transmit signal of 8.203 ms duration. In each case, the specified excitation range was from 511 718.75 Hz to 459 899.90 Hz (90 amu to 100 amu at 3.0 T). The spectra are as follows: (a) time-domain frequency sweep; (b) SWIFT with pseudorandom phase modulation of an originally specified rectangular magnitude spectrum; (c) as in (b), but with phase that is constant over the excitation bandwidth; (d) as in (b), but with quadratic phase modulation; (e) as in (d), but with apodization (Figure 6) of the stored time-domain waveform. Note the improved uniformity in excitation magnitude in (d) and (e) compared to (a).

half of the period, followed by a quarter-wave sinusoid for the final one-fourth of the period. This weight function is designed to force the time-domain signal smoothly to zero at the beginning and end of the time-domain period, while retaining the middle portion (in which most of the power is concentrated). After one zero fill, a magnitude-mode Fourier transform of the apodized time-domain signal gives a much flatter frequency-domain full spectrum (bottom left of Figure 6 or bottom right of Figure 5) than for the unapodized time-domain waveform (upper right of Figure 5 or lower right of Figure 2), without significant distortion.

Magnitude Uniformity for Various Experimentally Detected Excitation Spectra. Experimentally detected (via receive-during-transmit, with one zero fill to reveal the full spectrum) excitation magnitude spectra for several time-domain excitation waveforms are collected in Figure 7. It is worth noting that these profiles reflect the actual excitation power reaching the cell plates, including any nonlinearities from analog or digital manipulations along the way. Any of the SWIFT excitations based on continuous variation of phase across the spectrum clearly offers much-improved magnitude uniformity ("flat power") across the spectral excitation range, compared to frequency-sweep excitation. Constant-phase SWIFT is the least uniform in magnitude, because the aforementioned large time-domain dynamic range accentuates analog and digital nonlinearities. Quadratic phase encoding reduces the time-domain dynamic range and thus gives an experimental result that more closely approaches the specified input excitation spectrum. Time-domain apodization further smoothes the edges of the excitation magnitude spectrum.

Mass Selectivity. Figure 7 also shows that SWIFT excitation produces power with sharper cut-offs at the edges of the specified excitation frequency range, compared to frequency sweep excitation. Mass selectivity is even more improved when multiple excitation bands are needed. For example, Figure 8 shows what happens for simultaneous multiple-ion excitation (as for multiple-ion monitoring) of ions of 10 different m/z values. Frequency-sweep (or single-frequency excitation, not shown) would require 10 successive excitation events. (Since receive-during-transmit detection in our instrument requires a single excitation period, we generated a time-domain frequency-sweep waveform with 10 stepwise frequency ranges and then stored that waveform in our fast-memory module for subsequent recall in a single excitation period.) For the same total excitation period (8.203 ms), SWIFT offers much more selective excitation at the 10

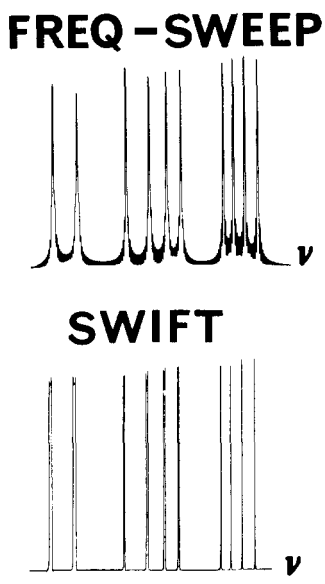

Figure 8. Experimental magnitude-mode excitation spectra for multiple-ion ejection or excitation, obtained via Fourier transformation of a once zero-filled time-domain receive-during-transmit signal: (top) frequency-sweep excitation; (bottom) SWIFT excitation with frequency-domain phase modulation and time-domain apodization. Although both spectra required time-domain waveforms of the same duration, SWIFT clearly offers the more selective excitation.

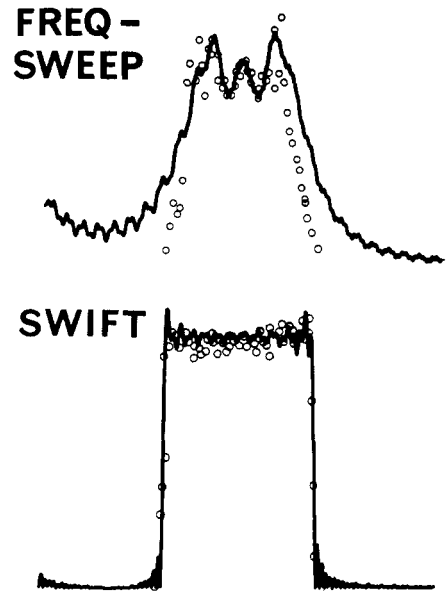

Figure 9. Experimental FT-ICR magnitude spectra for frequency-sweep (top) and SWIFT (bottom) excitation: (solid line) spectrum of the excitation itself, obtained via Fourier transformation of the time-domain receive-during-transmit signal; (circles) spectrum of the FT-ICR heterodyne response, as determined from ICR peak height at m/z 133 ($^{12}C_2{}^{35}Cl_2{}^{37}ClH_2{}^+$) relative to m/z 131 ($^{12}C_2{}^{35}Cl_3H_2{}^+$), as the rf carrier frequency is varied while the heterodyne bandwidth is kept constant (see text).

specified m/z values. The primary reason is that the SWIFT waveform is turned on and off just once, whereas the frequency-sweep (or single-frequency) signal must be turned on and off for each excited m/z range. Thus, any one component of the frequency-sweep is "on" for only one-tenth of the total excitation period (0.8203 ms in this case), and its magnitude spectrum is thereby 10 times broader at the edges. The experimentally detected magnitude mode power spectra in Figure 8 were obtained under the same experimental conditions as for Figure 7. At sufficiently low pressure in the cell, phase-modulated SWIFT is mass selective to within a frequency difference corresponding to one to three data points in the originally specified excitation spectrum. Thus, the ultimate mass selectivity for phase-modulated SWIFT excitation is limited only by the size of the stored-waveform data set and the pressure in the cell (so that ions remain trapped for as long as is required to excite them with the desired selectivity).

Experimental FT-ICR Response: SWIFT vs. Frequency-Sweep Excitation. We have previously demonstrated that FT-ICR performed with a cubic trapped-ion cell (*22*) is a highly linear system, in the sense that the amplitude of the response (i.e., peak intensity) is linearly proportional to the amplitude of the excitation (*23*). If the system is indeed linear, then the excitation magnitude spectrum applied to the ICR cell plates should be mirrored in the FT-ICR response measured from the signal induced on the cell plates from the coherent motion of the excited ions. Figure 9 shows the *excitation* magnitude spectra for frequency-sweep (top) and SWIFT (bottom) waveforms, measured at the ICR cell plates via receive-during-transmit detection (solid lines). The FT-ICR heterodyne-mode *response* was then determined by recording the relative ICR peak height for $^{12}C_2{}^{35}Cl_2{}^{37}ClH_2{}^+$ at m/z 133 in an electron-ionized sample of 1,1,1,2-tetrachloroethane, as the carrier frequency for the excitation was shifted by 40-Hz increments across the spectral range of interest. In order to compensate for scan-to-scan fluctuations in (e.g.) ion number, the m/z 133 peak height was ratioed to that for $^{12}C_2{}^{35}Cl_3H_2{}^+$ at m/z 131 in the same spectrum. The excitation magnitude spectrum therefore contained a narrow excitation band of interest (2075 Hz, specified by 34 data points) near m/z 133 and another wider band near m/z 131 so that the m/z 131 ions would be excited equally at all carrier offsets. Both frequency-sweep and SWIFT experiments were performed under the same conditions: 16.700 ms excitation period, 500 kHz bandwidth, and 16K time-domain data set, with signal-averaging (150 scans per spectrum) to enhance signal-to-noise ratio and average out scan-to-scan fluctuations. The spectra from the cell plates and the ICR response are not identical, because of analog and digital non-linearities and because the power reaching the reference ions at m/z 131 is not perfectly flat (and thus affects the peak height ratio between m/z 133 and m/z 131 as the carrier moves across the spectral range). Nevertheless, the response and excitation spectra are highly similar, and it is clear that phase-modulated SWIFT excitation provides flatter, more selective power across the specified m/z range, compared to frequency-sweep excitation.

Longitudinal Excitation. Although the above discussion and experiments have been limited to *transverse* (with respect to the applied magnetic field direction) excitation, the same SWIFT techniques could be used to eject ions in the *longitudinal* direction in either ICR or ion-trap (*24*) mass spectrometers. Of course, mass selectivity will be inherently poorer for longitudinal than for transverse excitation, because the "trapping" frequencies (*25*) are orders of magnitude smaller than ICR frequencies at typical magnetic field strengths (3–8 T). Nevertheless, phase-modulated SWIFT excitation should prove especially useful for multiple-ion ejection in ion-trap mass spectrometry, because SWIFT excitation can be designed with zero-power "windows", whereas ion ejection via ramping of the dc voltage in an ion-trap can eject ions only up to an upper m/z limit (*26*).

SUMMARY

In this paper, we have tried to show that stored waveform excitation works best when the time-domain dynamic range is kept small. However, SWIFT excitation designed to cover a wide frequency bandwidth can yield a time-domain waveform of large dynamic range. For an initially specified frequency-domain excitation magnitude spectrum, any of several

nonlinear continuous phase-modulations can reduce the time-domain dynamic range to a limit that approaches that for a frequency-sweep excitation. The best schemes are based upon continuous (rather than, e.g., pseudorandom) phase variation, and we find it convenient to use quadratic phase encoding in which the maximum rate of change of phase with frequency is kept to about half of the Nyquist limit of π radians per frequency-domain data point, so that the time-domain power is concentrated over about half of the time-domain waveform obtained via inverse Fourier transformation of the phase-encoded excitation magnitude spectrum. Apodization of the SWIFT time-domain waveform further smoothes the final frequency-domain excitation magnitude spectrum. Finally, SWIFT excitation includes all prior excitation waveforms as subsets and offers n-fold improvement (compared to multiple frequency-sweep excitation) in mass selectivity for excitation or ejection of ions of n distinct m/z ranges.

ACKNOWLEDGMENT

The authors wish to thank S. Goodman, A. Hanna, and M. B. Comisarow for helpful discussions.

LITERATURE CITED

(1) Comisarow, M. B.; Marshall, A. G. *Chem. Phys. Lett.* **1974**, *25*, 282-283.
(2) Comisarow, M. B.; Marshall, A. G. *Chem. Phys. Lett.* **1974**, *26*, 489-490.
(3) Marshall, A. G. *Acc. Chem. Res.* **1985**, *18*, 316-322.
(4) Gross, M. L.; Rempel, D. L. *Science (Washington, D.C.)* **1984**, *226*, 261-268.
(5) Wanczek, K. P. *Int. J. Mass Spectrom. Ion Processes* **1984**, *60*, 11-60.
(6) Freiser, B. S. *Talanta* **1985**, *32*, 697-708.
(7) Laude, D. A., Jr.; Johlman, C. L.; Brown, R. S.; Weil, D. A.; Wilkins, C. L. *Mass Spectrom. Rev.* **1986**, *5*, 107-166.
(8) Russell, D. H. *Mass Spectrom. Rev.* **1986**, *5*, 167-189.
(9) Comisarow, M. B. *Transform Techniques in Chemistry*; Griffiths, P. R., Ed.; Wiley: New York, 1986; pp 257-284.
(10) Nibbering, N. M. M., 10th International Conference on Mass Spectrometry, Swansea, Wales, Sept 1985 (text published in *Mass Spectrometry Advances*; Todd, J. F. J., Ed.; Wiley: New York, 1986).
(11) Marshall, A. G.; Roe, D. C. *J. Chem. Phys.* **1980**, *73*, 1581-1590.
(12) Marshall, A. G.; Wang, T.-C. L.; Ricca, T. L. *Chem. Phys. Lett.* **1984**, *108*, 63-66.
(13) Ijames, C. F.; Wilkins, C. L. *Chem. Phys. Lett.* **1984**, *108*, 58-62.
(14) Marshall, A. G.; Wang, T.-C. L.; Ricca, T. L. *J. Am. Chem. Soc.* **1985**, *107*, 7893-7897.
(15) Wang, T.-C. L.; Ricca, T. L.; Marshall, A. G. *Anal. Chem.* **1986**, *58*, 2935-2938.
(16) Marshall, A. G. *Physical Methods in Modern Chemical Analysis*; Kuwana, T., Ed.; Academic: New York, 1983; pp 57-135.
(17) Tomlinson, B. L.; Hill, H. D. W. *J. Chem. Phys.* **1973**, *59*, 1775.
(18) Blümich, B. *Bull. Magn. Reson.* **1985**, *7*, 5-26.
(19) Bertholdi, E.; Ernst, R. R. *J. Magn. Reson.* **1973**, *11*, 9.
(20) Comisarow, M. B.; Melka, J. D. *Anal. Chem.* **1979**, *51*, 2198-2203.
(21) Bracewell, R. N. *The Fourier Transform and Its Applications*, 2nd ed.; Brown, J. V., Gardner, M., Ed.; McGraw-Hill: New York, **1978**, pp 104-107.
(22) Comisarow, M. B. *Int. J. Mass. Spectrom. Ion Phys.* **1981**, *37*, 241.
(23) Marshall, A. G.; Wang, T.-C. L.; Ricca, T. L. *Chem. Phys. Lett.* **1984**, *105*, 233.
(24) Fulford, J. E.; March, R. E.; Mather, R. E.; Todd, J. F. J.; Waldren, R. M. *Can. J. Spectrosc.* **1980**, *25*, 85-97.
(25) Jeffries, J. B.; Barlow, S. E.; Dunn, G. H. *Int. J. Mass Spectrom. Ion Processes* **1983**, *54*, 169-187.
(26) Kelley, P. E.; Stafford, G. C., Jr.; Syka, J. E. P.; Reynolds, W. E.; Louris, J. N.; Todd, J. F. J. American Society for Mass Spectrometry 33rd Annual Conference on Mass Spectrometry and Applied Topics, San Diego, CA, May 1985; pp 707-708.

RECEIVED for review July 24, 1986. Accepted October 1, 1986. This work was supported by grants (to A.G.M.) from the U.S.A. Public Health Service (NIH GM-31683) and The Ohio State University.

In Vivo Mass Spectrometric Determination of Organic Compounds in Blood with a Membrane Probe

Jennifer S. Brodbelt and R. Graham Cooks*

Department of Chemistry, Purdue University, West Lafayette, Indiana 47907

James C. Tou,* George J. Kallos, and Mark D. Dryzga

Analytical Laboratories, Dow Chemical U.S.A., Midland, Michigan 48640

An improved intravenous membrane probe, using hollow fiber silicon tubing, is used for in vivo mass spectrometric blood analysis. Detection limits in blood (in vitro) are 1 ppm or less for dichloromethane, methoxyflurane, and styrene. Response times are several minutes. Inhalation of dichloromethane or methoxyflurane by a rat is detected by monitoring the compound in the blood. The concentration of dichloromethane was monitored in vivo and found to fall exponentially (k = -0.15 min^{-1}).

The analysis of biological fluids for exogenous organic compounds, including drugs and their metabolites, is of interest to chemists and toxicologists (*1-4*). Currently accepted techniques for the study of organics in blood are gas and liquid chromatography, utilized in conjunction with sensitive detection systems such as flame ionization, mass spectrometry, or electrochemical detection (*5-7*). Although these techniques display good detection limits, they often require extensive sample preparation and do not allow direct in vivo measurements. Furthermore, for studies involving exposure of animals to potentially toxic compounds, blood samples must be withdrawn on a periodic basis with deleterious effects on the animals.

Recently, there has been a surge in applications of membranes as separators in a wide variety of analytical determinations (*8-20*). Several investigators have used membrane separation in conjunction with mass spectrometry, typically to allow the selective sampling and characterization of relatively volatile compounds from aqeous solutions containing complex mixtures (*10-20*). Although membranes are sometimes employed as sheets, the use of hollow fibers is an attractive alternative. These can be fashioned into probes which

0003-2700/87/0359-0454$01.50/0